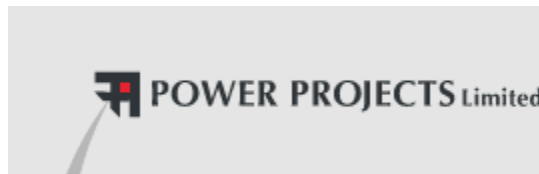


HYDRODYNAMIC OPTIMISATION OF A POINT WAVE-ENERGY CONVERTER USING LABORATORY EXPERIMENTS

by

Scott Kelly

with support from



THE UNIVERSITY
OF AUCKLAND

NEW ZEALAND

Te Whare Wananga o Tamaki Makaurau

A thesis submitted in partial fulfilment of the requirements for the degree of Master of Civil Engineering, The University of Auckland, February 2007.

Summary

Investment in renewable energy technology, such as wave power, is increasingly seen as a beneficial and economically-viable alternative to existing fossil-based power plants. New Zealand has particularly energetic ocean waves and is well positioned to harness wave energy as a source of power. This thesis presents an in-depth analysis of scale-model experiments conducted on a novel WEC (Wave Energy Converter) device called the 'spar fork'. The model was built using Froude scaling, with a dimensional scale ratio of 1:25 between model and prototype.

Tests were performed on the device in a 20m long wave flume, with waves being created and measured in the flume using a specially designed control system created in LabVIEW 8.0. Wave flume operation was validated by showing strong correlation between experimental results and dispersion theory. Sub-surface velocity profiles were shown to compare well with Stokes' Second Order theory. Wave reflection analysis showed that reflected wave heights for the newly-installed flume beach were approximately 5% of the total wave height, which is well inside the acceptable range for wave flume modelling - that is, less than 10%.

Friction-torque for the spar fork model (representing the generator resistance of the prototype) was evaluated using pendulum decay methods. With software developed in MATLAB, angular velocities of the moving parts of the spar fork were measured using image processing and particle tracking methods. From the measurements taken, the power generated could be calculated for a number of wave states, also providing the opportunity to test a number of spar fork configurations.

It was found that the optimum spar fork design will include a significantly buoyant spar section tightly moored to the sea floor by no less than two mooring lines. The arm of the spar fork was optimum when its length was equal to the wave height. It is recommended that active float size is also maximised, as both these variables increase the amount of torque that can be generated. Designing the spar to be of natural heave frequency less than, but approaching the frequency of the design wave climate is particularly advantageous for power generation (although challenging physically). Further device recommendations are given in the conclusions.

For the expected wave climate on the west coast of New Zealand (using significant wave properties), the total power output of the tested device is shown to increase from 2.2kW for the original design to 5.4kW after optimisation.

Acknowledgements

It is my belief that society will one day meet all of its energy needs with sustainable resources. With this in mind, I dedicate this thesis to future generations who will depend on such technologies.

Foremost, I would like to thank my supervisor, Associate Professor Stephen Coleman. Firstly, for having faith in my abilities to complete such an ambitious project and secondly for providing such a comprehensive review of my thesis. Thanks also for the academic reference that greatly assisted with my successful application for a scholarship and acceptance to do further study towards sustainable technology in the United Kingdom.

I would like to fully acknowledge the three organisations that have come together to make this study possible: NIWA, Power Projects Limited and Industrial Research Limited. These three organisations together formed a body called WET-NZ, successfully winning a grant through FRST to build a prototype wave-energy converter specifically designed for New Zealand's energetic oceans. I sincerely appreciate the opportunity that WET-NZ has provided, as it has given me the unique opportunity to do research in a field that I am passionate about.

Craig Stevens of NIWA, thanks for your ideas, hospitality, and thorough review of my work. Lan Le-Ngoc of Industrial Research Limited, thanks for always finding the time to explain new material in detail. Alistair Gardener of Industrial Research Limited, thanks for your enthusiasm and confidence. John Huckerby of Power Projects Limited, thanks for spear-heading wave energy conversion technology to the New Zealand government. If wave energy is to be taken seriously, there needs to be a regulatory environment to support it.

A special thanks to The University of Auckland Civil Engineering Fluids Laboratory technicians, Geoff Kirby and Jim. Y. Luo. Your technical assistance throughout the

project was invaluable. My research methodology and experimental apparatus would not have been possible without your help.

Lastly but most importantly, I would like to acknowledge and thank my partner, Bec France, my closest friend and true love. Beccs, it is your enduring support and confidence that has allowed me to follow my dreams. I hope that one day I can return the favour.

Table of contents

LIST OF FIGURES	XV
LIST OF TABLES	XXI
NOMENCLATURE	XXIII
1 INTRODUCTION	1
1.1 Motivation	1
1.2 Call for sustainability	3
1.3 Using marine energy as a source of renewable power	6
1.4 Marine energy in New Zealand	8
1.5 Thesis overview	10
2 LITERATURE REVIEW	13
2.1 Methods of extracting energy from the ocean	14
2.1.1 Off-shore wind energy	14
2.1.2 Marine biomass	15
2.1.3 Salinity gradients	15
2.1.4 Ocean temperature gradients	16
2.1.5 Underwater thermal vents (geothermal)	17
2.1.6 Tidal energy	17
2.2 Methods of extracting energy from waves	19
2.2.1 Existing technology	20
2.2.2 Oscillating Water Column (OWC)	21
2.2.3 Overtopping devices	24
2.2.4 Wave activated devices	24
2.2.5 Closing remarks on wave energy conversion	27
2.3 Basic wave theory	28
2.3.1 Fundamental principles of surface waves	28
2.3.2 Ocean waves	28
2.3.3 How wind-generated waves are created	29
2.3.4 Wave properties	31
2.3.5 Phase speed and wave group speed	33

2.3.6	Wave interference	34
2.3.7	Waves at the shoreline	35
2.3.8	Refraction reflection and diffraction	36
2.4	Hydrodynamic wave theory	37
2.4.1	Water particle kinematics	37
2.4.2	Pressure field	40
2.4.3	Wave energy	40
2.4.4	Energy flux	42
2.5	Definition of real wave properties	43
2.5.1	Wave spectra	43
2.6	Vibration theory	45
2.7	Image processing theory	50
2.7.1	Background	50
2.7.2	Digital particle tracking velocimetry	50
3	EQUIPMENT AND MEASURING METHODOLOGY	53
3.1	Dimensional analysis and similitude	54
3.1.1	Purpose of scale model	54
3.1.2	Spar fork model similitude	58
3.1.3	Adopted scale factors	58
3.1.4	Laboratory and scale effects	60
3.1.5	Length scale factor adopted	61
3.1.6	Morison equation and drag forces on submerged cylinders	62
3.2	Wave flume and measuring equipment	65
3.2.1	Wave flume and wave generator	65
3.2.2	Data acquisition control and measurement system	68
3.2.3	Capacitance wave probes and calibration	69
3.2.4	Calibration of wave probes	70
3.2.5	Equipment used for measurement of subsurface wave velocity profiles (Acoustic Doppler Velocimetry)	71
3.3	LabVIEW 8.0 Measurement and control software	72
3.3.1	Measurement and control of the wave flume using LabVIEW 8.0	72
3.3.2	Nyquist Frequency and sampling rates	73
3.3.3	Program capabilities and overview	74

3.3.4	Program description	77
3.4	Spar fork measurement and analysis equipment	78
3.4.1	Equipment used to measure friction-torque within the spar fork	78
3.4.2	Particle tracking	79
4	WAVE FLUME VALIDITY AND PERFORMANCE	81
4.1	Wave flume validation using wavelength calculations	82
4.1.1	Wavelength calculation overview	82
4.2	Validation using wave-reflection analysis	84
4.2.1	Wave-reflection analysis overview	84
4.2.2	Calculating wave reflection	85
4.2.3	Experimental procedure	89
4.2.4	Description of MATLAB processing	91
4.3	Validation using subsurface wave velocity profiles	93
4.3.1	Sub-surface velocity profile overview	93
4.3.2	Predicting subsurface wave velocity profiles using theory	94
4.3.3	Experimental procedure	97
4.4	Results	99
4.4.1	General wave profile recordings	99
4.4.2	Results for wavelength comparison	101
4.4.3	Results for wave reflection analysis	103
4.4.4	Subsurface wave velocity profile results	106
5	DESIGN AND DEVELOPMENT OF SPAR FORK	111
5.1	Early development of spar fork concept	112
5.2	Deployment location	113
5.3	Selection of wave spectra	114
5.4	Design conditions and constraints	115
5.4.1	The spar fork concept	116
5.4.2	Concepts for power generation for the prototype model	117
5.4.3	General operating principles and derivations	119
5.5	Methodological approach to optimise spar design	120
5.6	Device size and orientation	121
5.6.1	Dynamic analysis of active float	122

5.7	Description of spar fork variables to be tested	126
5.7.1	Internal resistance (friction-torque)	126
5.7.2	Main spar (reactive platform)	126
5.7.3	Mooring line resistance	126
5.7.4	Inertial resistance of main spar	127
5.7.5	Hydrodynamic resistance	128
5.7.6	Active float (buoyant float)	128
6	TEST PROCEDURES AND METHODOLOGIES	131
6.1	Methodology	132
6.2	Measurement of friction torque	133
6.2.1	Purpose and definition of friction-torque	133
6.2.2	Measuring friction torque using pendulum theory	134
6.2.3	Pendulum theory for large amplitudes	137
6.2.4	Experimental Procedure	138
6.2.5	Calculation of friction-torque using MATLAB	143
6.2.6	Modelling an under-damped pendulum using Matlab	146
6.2.7	Validation of coulomb damping effects	148
6.2.8	Buoyancy force and gravitational force relationship with coulomb damping	153
6.3	Particle tracking methods	154
6.3.1	Experimental methodology	154
6.3.2	Particle identification and tracing program	155
6.3.3	Image filtering	157
6.3.4	Particle detection and location	158
6.3.5	Particle tracking	159
6.3.6	Analysing results	161
6.3.7	Changing co-ordinate system relative to joint	162
6.3.8	Changing from Cartesian to polar co-ordinate system	164
6.3.9	Removing particle location error	165
6.3.10	Using numerical methods to determine the angular velocities and angular accelerations of the particles	168
6.3.11	Fitting a smoothing spline to find derivatives from the experimental data	169
6.3.12	Calculating mean power absorbed	171
6.3.13	Validity of particle tracking methods	173

7	HYDRODYNAMIC PROPERTIES OF VERTICAL SPARS UNDER WAVE EXCITATION	175
7.1	Definition of some geometric and dynamic parameters of spar buoys	176
7.1.1	Geometric parameters	176
7.1.2	Dynamic parameters	177
7.2	Unforced hydrodynamic response of structures and objects in water	178
7.2.1	Dynamic effects on spar buoys	178
7.2.2	Hydrostatic buoyancy stiffness	179
7.2.3	Hydrodynamic damping factor	182
7.2.4	Hydrodynamic added mass effect	182
7.2.5	Unforced hydrodynamic heave motion	183
7.3	Forced hydrodynamic response of structures and objects in water	184
7.3.1	Natural frequency, phase difference and vibration theory	185
7.4	Motion of a damped natural oscillator in water	189
7.5	Experimental procedure	191
7.5.1	The unforced dynamic response of a vertical cylinder	193
7.6	Results for free decay tests in still water	195
7.6.1	Response of cylinder at the heave natural frequency	198
7.6.2	Response of cylinder at the pitch natural frequency	200
7.6.3	Response of vertical cylinder to excitation	203
7.7	Spar fork modifications to match wave climate	207
7.7.1	Testing implications for spar fork design	207
7.7.2	Optimisation of geometries	209
8	RESULTS FOR THE TESTING AND OPTIMISATION OF SPAR FORK DESIGN	217
8.1	Variations made to main spar structure	220
8.1.1	Original concept	220
8.1.2	Main spar buoyancy properties	220
8.1.3	Attaching a vertical damping plate to the main spar section	224
8.2	Mooring lines	227
8.2.1	Mooring line attachment to spar fork	227

8.2.2	Mooring line configurations	229
8.3	Active float properties	232
8.3.1	Active float parameters	232
8.3.2	Active float arm length	233
8.3.3	Active float size and buoyancy	236
8.4	Effects of ocean current on spar fork performance	237
8.5	Resonant spar buoy with active float	238
8.6	General discussion about overall results	239
9	CONCLUSIONS AND RECOMMENDATIONS	241
9.1	Wave validation and control	242
9.2	Experimental methodology of spar fork	244
9.3	Hydrodynamic response of an oscillating spar	245
9.4	Maximising power output of spar fork	247
9.5	Concluding remarks and work still to be completed on the spar fork	250
	REFERENCES	253
	APPENDIX A-1: SPAR FORK RESULTS	259
	APPENDIX A-2: WAVE LENGTH VALIDATION	289
	APPENDIX A-3: RESULTS FOR FOURIER ANALYSIS	291
	APPENDIX A-4: RESULTS FOR SUB-SURFACE VELOCITY PROFILES	293
	APPENDIX B-1: 'SPARPOWER.M'	301
	APPENDIX B-2: 'INITIALISE.M'	308
	APPENDIX B-3: 'WAVEVEL.M'	309
	APPENDIX B-4: 'TANKREFLECTIONS.M'	312
	APPENDIX B-5: 'PENDULUM.M'	315
	APPENDIX B-6: 'MOVFINAL.M'	320
	APPENDIX B-7: LABVIEW MEASUREMENT CONTROL OF WAVE FLUME	322
	APPENDIX C-1: HYDRODYNAMIC PROPERTIES OF CYLINDER 1	323
	APPENDIX C-2: HYDRODYNAMIC PROPERTIES OF CYLINDER 2	326
	APPENDIX D-1: DVD-ROM CONTAINING RESULTS AND DOCUMENTATION	330

List of figures

Figure 1.1:	The world's energy usage as a percentage by source for 1973 and 2004	3
Figure 1.2:	Evolution of the world's energy supply 1971 – 2004.....	3
Figure 1.3:	Oil produced by country since 1900	4
Figure 1.4:	Wave energy abundance on the coastlines around the world.....	7
Figure 2.1:	Offshore wind farm.....	15
Figure 2.2:	Ocean depth temperature gradients	17
Figure 2.3:	World tectonic plate locations	17
Figure 2.4:	Tidal energy devices	19
Figure 2.5:	Classification of wave energy conversion processes	21
Figure 2.6:	Oscillating water column working principles	22
Figure 2.7:	Two operating examples of the oscillating water column wave energy device.....	22
Figure 2.8:	Offshore oscillating water column devices	23
Figure 2.9:	Prototype image of the onshore Wave-mill device	23
Figure 2.10:	Three examples of overtopping type wave energy converters	24
Figure 2.11 :	Photo of the Pelamis wave energy converter	25
Figure 2.12:	Three examples of point absorber devices	26
Figure 2.13:	Two examples of wave energy farms.....	27
Figure 2.14:	Energy distribution of waves within the ocean	29
Figure 2.15 :	Generation of waves from wind.....	30
Figure 2.16:	Properties of subsurface wave profiles showing circular motion of wave particles.....	31
Figure 2.17:	Surface profile of real ocean waves	32
Figure 2.18:	Subsurface particle motion.....	33
Figure 2.19:	Wave interference patterns.....	34
Figure 2.20:	How a wave breaks on the shore	35

Figure 2.21: Refraction of waves	36
Figure 2.22: Acceleration and velocity of particle motions under the surface of a wave	37
Figure 2.23: Experimental particle image velocimetry setup	51
Figure 3.1: Graphical comparison of scaling laws	56
Figure 3.2 : Wave maker and hydraulic ram	66
Figure 3.3 : General setup of the wave flume control and measurement system	67
Figure 3.4: Signal generator and control box for wave flume	68
Figure 3.5: Data acquisition card	68
Figure 3.6: Capacitance measurement probe	69
Figure 3.7: Signal amplification box	70
Figure 3.8: Micro ADV setup	72
Figure 3.9: Screen shot of GUI created in LabVIEW 8.0 used to display and record information about the waves being generated	75
Figure 3.10: Screen-shot of GUI created in LabVIEW 8.0 used to control the wave maker	76
Figure 3.11: LABJACK U12	78
Figure 3.12: Screen shot of DAQFactory Express (pendulum decay)	79
Figure 3.13: Diagram showing the setup used for tracking particles on the spar fork	80
Figure 4.1: Placement of probes in the wave flume for wave reflection analysis	87
Figure 4.2: Fourier transform power spectrum	89
Figure 4.3: Fourier fitted model and experimental data	92
Figure 4.4: Regions of validity for various wave theories	95
Figure 4.5 : Differences in wave profiles for linear and second-order theories	96
Figure 4.6: Wave profile recordings for a depth of 700mm	100
Figure 4.7: Wave profile recordings for a depth of 750mm	100
Figure 4.8: Wave profile recording for a depth of 800mm	101
Figure 4.9: Example non-linearities in the wave profile recorded in the flume at low frequencies	101

Figure 4.10:	Wavelength comparison for dispersion theory and experimental results:.....	102
Figure 4.11:	Wavelength comparison for dispersion theory and experimental results:.....	102
Figure 4.12:	Wave reflection analysis: old beach	104
Figure 4.13:	Wave reflection analysis: new beach.....	104
Figure 4.14:	Example of higher order harmonics that exist within the wave flume	105
Figure 4.15:	Fourier analysis of recorded wave profile (H = 160 mm)	106
Figure 4.16:	Subsurface horizontal wave velocity profile at sevens levels	107
Figure 4.17:	Subsurface horizontal wave velocity profile for min/max probe levels (Table 4.2).....	107
Figure 4.18:	Subsurface vertical wave velocity profile at sevens levels (Table 4.2).....	108
Figure 4.19:	Subsurface vertical wave velocity profile for min/max probe levels	108
Figure 5.1:	Time series plots of wave-rider buoy data showing significant wave height and significant wave period at Banks Peninsula, New Zealand	113
Figure 5.2:	Average significant wave height (m) around New Zealand 1979-98	114
Figure 5.3:	Bretschneider spectrum for modelled conditions	115
Figure 5.4:	Original spar fork design (Author: Craig Stevens).....	117
Figure 5.5:	Modes of motion during spar fork operation.....	119
Figure 5.6:	Flow diagram showing design process adopted	121
Figure 5.7:	Free body diagram of active float.....	122
Figure 6.1:	Natural decay of an under-damped pendulum	137
Figure 6.2:	Relationship between change in relative period and amplitude release height for a standard	138
Figure 6.3:	Spring configuration and fluorescent dot.....	139
Figure 6.4:	Experimental setup for calculating coulomb friction within the joint	139
Figure 6.5:	Increase in pendulum length for the measurement of coulomb friction	141

Figure 6.6:	Experimentally-recorded results for three repeated measurements for an underdamped sinusoidal pendulum motion	143
Figure 6.7	Experiment (i) decay of pendulum motion without spring compression forces.....	144
Figure 6.8:	Experiment (ii) decay of pendulum motion with spring compression forces applied at joint.....	145
Figure 6.9:	Comparison between Matlab generated LTI model and experimental results.....	146
Figure 6.10:	Comparison between results of MATLAB generated LTI model and the system of equations used to define pendulum motion	147
Figure 6.11:	Coulomb damping vs viscous damping validation	149
Figure 6.12:	Example of loop written in MATLAB	150
Figure 6.13:	Three dimensional matrix storing error values for particular sets of values of three unknown quantities.....	151
Figure 6.14:	Pendulum decay using numerical methods	152
Figure 6.15:	Flow diagram representing the methodological process used in MATLAB for particle tracking analyses	156
Figure 6.16:	Preparation of frames using image processing	158
Figure 6.17:	Binary and graphical representation of particle.....	159
Figure 6.18:	Example showing particle tracks for a single experiment.....	160
Figure 6.19:	Plot of the interpolation of the particle locations	162
Figure 6.20:	Particle Cartesian co-ordinates relative to top left corner of frame	163
Figure 6.21:	Particle co-ordinates relative to generator [particle (2)]	163
Figure 6.22:	Representation of the four-quadrant inverse tangent.....	165
Figure 6.23:	Particle location shown in polar co-ordinates relative to Particle (2)	165
Figure 6.24:	Measured distances of Particle (1) and Particle (3) relative to Particle (2).....	167
Figure 6.25:	Measured distances of Particle (1) and Particle (3) relative to Particle (2).....	167
Figure 6.26:	Plot of the derivative of the relative y position of Particle (1) showing noisy data	169

Figure 6.27: Best fit approximation of data using Matlab smoothing spline with 99% accuracy	170
Figure 6.28: Experimental angular displacement, fitted angular displacement, angular velocity and calculated angular acceleration for a data set.	171
Figure 6.29: Plot showing the relative angular displacement, relative velocity and relative angular acceleration for the spar fork.....	172
Figure 6.30: Predicted power output from spar fork.....	172
Figure 6.31: Particle tracks for a spar with arms locked in relative position	174
Figure 6.32: Relative motion between arms for a spar with a locked joint.....	174
Figure 7.1: Geometric properties of spar buoy	177
Figure 7.2: Definitions of motion in six degrees of freedom	178
Figure 7.3: Photo of cylinders used for spar-response experimentation	192
Figure 7.4: Definitions of spar geometric properties	194
Figure 7.5: Response of Cylinder one to a free decay test.....	198
Figure 7.6: Theoretical heave amplitude response plotted using values from experiments	199
Figure 7.7: Phase angle ε between cylinder and wave	200
Figure 7.8: Variation of pitch natural frequency with metacentric height	203
Figure 7.9: Motion of cylinder in response to propagating wave frequency	205
Figure 7.10: Response of spar optimised for heave resonance	206
Figure 7.11: Bretschneider Spectrum superimposed on response for cylinders	208
Figure 7.12: Spar with disk inducing added mass effect.....	210
Figure 7.13: Heave response of optimised cylinders at various wave frequencies shown relative to the Bretschneider spectrum.....	214
Figure 7.14 : Phase angle of optimised cylinders at various wave frequencies shown relative to the	215
Figure 8.1: Overview and explanation of results included in Appendix A-1	219
Figure 8.2: Relative angular motion between active float and main spar.....	221
Figure 8.3: Mooring line and buoyancy forces for a spar fork at neutral position	222

Figure 8.4:	Buoyancy and mooring line forces for the spar fork at a wave trough	223
Figure 8.5:	Relative angular displacement between main spar and active float for neutral buoyancy and large buoyancy over multiple wave states.....	223
Figure 8.6:	Buoyancy and mooring line forces for a spar fork at a wave peak	224
Figure 8.7:	Vertical damping plate	225
Figure 8.8:	Power output variation with damping plate location (water depth = 800mm)	226
Figure 8.9:	Power output variation for case of high friction torque (also compares the effect of current on a damping plate)	227
Figure 8.10:	Mooring line attachment locations.....	227
Figure 8.11:	Mooring line attachment location effects on power output and maximum relative angular displacement (water depth = 800mm).....	228
Figure 8.12:	Plan view of mooring line configurations tested.....	229
Figure 8.13:	Effects of mooring line configuration (water depth = 800mm).....	230
Figure 8.14:	Spar fork showing horizontal attachment plate for configuration (i)	231
Figure 8.15:	Particle tracks for Configurations (iv) and (v)	231
Figure 8.16:	Power output for a spar fork with a long arm and large float.....	233
Figure 8.17:	Comparison of relative angular velocities for spar forks with the same medium friction level	234
Figure 8.18:	Power absorbed for short and long arm lengths at medium friction	235
Figure 8.19:	Effects of float size on mean absorbed power and maximum relative angular displacement	236
Figure 8.20:	Effects of ocean currents on mean absorbed power and maximum relative angular displacement (just waves – spar fork 8, waves and current - spar fork 22)	238
Figure 8.21:	Spar fork designed to resonate with propagating wave frequency	239
Figure 9.1:	Diagram of LabVIEW program for controlling wave flume	320

List of tables

Table 3.1:	Common dimensionless ratios associated with wave mechanics and their descriptions	55
Table 3.2:	Complete set of scale factors using Froude scaling.....	59
Table 3.3:	Prototype and scale model dimensions.....	62
Table 3.4:	Morison coefficients suggested by Clauss (1992).....	65
Table 3.5:	Data acquisition card properties	68
Table 3.6:	LABJACK U12 specifications	78
Table 4.1:	Wave profile experimental data-sets	90
Table 4.2:	Micro ADV recorded data-sets (water depth = 800 mm).....	99
Table 7.1:	Properties of cylinders tested.....	194
Table 7.2:	Summary of results for Cylinder one	196
Table 7.3:	Summary of results for Cylinder two	196
Table 7.4:	Values for spar buoys tested in pitch.....	201
Table 7.5:	Properties of cylinders when pitching motion would dominate.....	202
Table 7.6:	Constraints used for optimisation of cylinder properties	211
Table 7.7:	Optimised solution for four different geometric scenarios of prototype	212
Table 8.1:	Summary of results for spar forks tested using significant wave properties ($\omega=2\text{rads}^{-1}$ $H_s=120\text{mm}$).....	218
Table 8.2:	Location in Appendix A-1 for the summary of results of mooring line configurations.....	230
Table 8.3:	Location in Appendix A-1 for the summary of results for medium friction and arm length.....	234



Nomenclature

Variables used to define waves

k	angular wave number ($2\pi / \lambda$)
x	horizontal displacement from frame of reference (m)
a_i	incident wave amplitude (m)
F_0	magnitude of the force created from a wave (N)
H_{\max}	maximum wave height (m)
p	pressure (Pa)
a_r	reflected wave amplitude (m)
H_s	significant wave height (m)
T_s	wave period (s)
\bar{T}	significant wave period (s)
a_x	subsurface horizontal wave particle acceleration (ms^{-2})
u	subsurface horizontal wave particle velocity (ms^{-1})
u_0	subsurface horizontal wave amplitude particle velocity (ms^{-1})
a_y	subsurface vertical wave particle acceleration (ms^{-2})
w	subsurface vertical wave particle velocity (ms^{-1})
y	vertical displacement from the still water level (m)
h	water depth (m)
A	wave amplitude
ω	wave angular frequency (rads^{-1})
f	wave frequency (s^{-1})
V_g	wave group speed (ms^{-1})
H	wave height (m)
λ	wave length (m)
M, M_0	wave moments (N.m)
T	wave period (s)
v	wave phase speed or wave celerity (ms^{-1})
η	wave surface profile from still water level (m) (also used to represent efficiency)

Common variables

m_a	added mass (kg)
\hat{I}_{yy}	area moment of inertia (m ⁴)
u	breach height above the still water level of object (m)
$L_{m,p}$	characteristic length of model/prototype (m)
ω_d	damped natural frequency (rads ⁻¹)
T_d	damped period (s)
ρ	density of water (998 kgm ⁻³)
D_d	diameter of disc (m)
ξ	dimensionless damping factor
ζ	distance between wave capacitance probes (m)
F_d	drag force (N)
τ_f	friction torque (N.m)
L, r, d	geometric properties of object (length, radius, distance) (m)
g	gravitational constant (ms ⁻²)
F_g	gravitational force (N)
$\nu_{m,p}$	kinematic viscosity of model/prototype (m ² s ⁻¹)
E_K	kinetic energy (J)
l	length of pendulum (m)
δ	logarithmic decrement for an exponentially decaying pendulum (also used by Isaacson (1991) to represent the phase difference between probes)
m	mass (kg)
I	mass moment of inertia (N.s ² .m)
P_{\max}	maximum possible power achievable (W)
ω_n	natural frequency (rads ⁻¹)
$\omega_{n,p}$	natural frequency in pitch (rads ⁻¹)
σ	phase difference between the wave and the wave force (rad) (also used to represent the statistical quantity of standard deviation)
τ	phase difference between an object and a wave (rad)
ε	phase difference between an object relative to a wave (rad)
E_P	potential energy (of a wave) (J)
U_T	potential energy (of a pendulum) (J)
P	power (W)
θ_R	relative angular displacement of between arms on the spar fork (rad)
Δ	release height of pendulum (deg)
α	scale factor ratio (usually with subscript 'L' designating length)
c	spring stiffness (modulus) (N.m ⁻¹)

$c_{\theta\theta}$	spring stiffness in pitch ($\text{N}\cdot\text{m}^{-1}$)
U_0	subsurface velocity amplitude (ms^{-1})
t	time (s)
E_T	total energy contained within a wave (kinetic plus potential)
a	virtual mass ($m_a + m$) (kg)
b	viscous damping coefficient ($\text{N}\cdot\text{sm}^{-1}$)
F_v	viscous force (N)
∇	volume (m^3)
A_w	water plane area (m^2)
U	wave flume current (ms^{-1})
\mathbf{W}_T	work (J)

